NATIONAL ADVISORY COMMITTEE FOR AERONAUTICS

TECHNICAL NOTE

No. 1286

LOW-SPEED STABILITY AND DAMPING-IN-ROLL CHARACTERISTICS OF SOME HIGHLY SWEPT WINGS

By Bernard Maggin and Charles V. Bennett

Langley Memorial Aeronautical Laboratory
Langley Field, Va.

Washington
May 1947

NATIONAL ADVISORY COMMITTEE FOR AERONAUTICS

TECHNICAL NOTE No. 1286

LOW-SPEED STABILITY AND DAMPING-IN-ROLL CHARACTERISTICS OF SOME HIGHLY SWEPT WINGS

By Bernard Maggin and Charles V. Bennett

SUMMARY

Tests have been conducted to determine the low-speed stability, damping-in-roll, and stall characteristics of five wings, three wings with 42° sweepback and having aspect ratios of 5.9, 3, and 2, and two wings with 38° sweepforward and having aspect ratios of 5.9 and 3. The results showed that the wings of aspect ratio 5.9 were longitudinally unstable at the stall but that reducing the aspect ratio tended to eliminate the instability. Sweepforward produced a maximum value of negative effective dihedral approximately one-half of the positive value produced by sweepback. Over the linear range of the lift curve the swept-forward wings had zero directional stability, whereas the swept-back wings had a marked increase in directional stability with lift coefficient. The damping in roll was reduced with reduction in aspect ratio over the linear range of the lift curve. Above the linear range of the lift curve the damping in roll decreased with increasing lift coefficient for the swept-back wings and increased with increasing lift coefficient for the swept-forward wings. Autorotation at the stall was obtained only with the swept-back wing having an aspect ratio of 2.

INTRODUCTION

An investigation to determine the low-speed stability and control characteristics of highly swept wing plan forms is being conducted in the Langley free-flight tunnel and in the Langley 15-foot free-spinning tunnel. Some results of damping-in-roll tests, force tests, free-flight tests, and tuft tests of these wings are presented in references 1 and 2. In the present paper, results are given of experimental investigations conducted to determine the low-speed stability, damping-in-roll, and stall characteristics of five wings, three wings with 42° sweepback and having aspect ratios of 5.9, 3, and 2, and two wings with 38° sweepforward and having aspect ratios of 5.9 and 3.

SYMBOLS

A	aspect ratio
S	wing area, square feet
q	dynamic pressure, pounds per square foot
V	airspeed, feet per second
b	wing span, feet
$\bar{c}$	mean aerodynamic chord measured in plane parallel to plane of symmetry, feet
λ	taper ratio, tip chord divided by root chord
Λ	angle of sweep of the quarter-chord line of the wing, degrees (positive, sweepback; negative, sweepforward)
α	angle of attack, degrees
β	angle of sideslip, degrees
ψ	angle of yaw, degrees; for force tests, $\psi = -\beta$
ϕ	angle of roll, degrees
L	rolling moment, foot-pounds
M	pitching moment, foot-pounds
N	yawing moment, foot-pounds
C_L	lift coefficient $\left(\frac{\text{Lift}}{qS}\right)$
C_D	drag coefficient $\left(\frac{\text{Drag}}{qS}\right)$
C_m	pitching-moment coefficient $\left(\frac{\text{Pitching moment}}{qS\bar{c}}\right)$
C_l	rolling-moment coefficient $\left(\frac{\text{Rolling moment}}{qSb}\right)$

C_n yawing-moment coefficient $\left(\frac{\text{Yawing moment}}{qSb}\right)$

C_Y lateral-force coefficient $\left(\frac{\text{Lateral force}}{qS}\right)$

C_{l_β} effective-dihedral parameter $\left(\frac{\partial C_l}{\partial \beta}\right)$; rate of change of rolling-moment coefficient with angle of sideslip, per degree

C_{n_β} directional-stability parameter $\left(\frac{\partial C_n}{\partial \beta}\right)$; rate of change of yawing-moment coefficient with angle of sideslip, per degree

C_{Y_β} lateral-force parameter $\left(\frac{\partial C_Y}{\partial \beta}\right)$; rate of change of lateral-force coefficient with angle of sideslip, per degree

$\frac{pb}{2V}$ helix angle generated by wing tip in roll, radians

C_{l_p} damping-in-roll parameter $\left(\frac{\partial C_l}{\partial \frac{pb}{2V}}\right)$; rate of change of rolling-moment coefficient with helix angle generated by wing tip

APPARATUS AND TESTS

The geometric characteristics of the five models used in the present tests are given in figure 1. Three of the wings had 42° sweepback and aspect ratios of 5.9, 3, and 2, and two of the wings had 38° sweepforward and aspect ratios of 5.9 and 3. These plan forms were obtained by rotating the basic wing of reference 1 ($A = 10$, $\Lambda = 2°$, $\lambda = 0.5$) about the 0.50-root-chord point to the desired sweep angle of the quarter-chord line. For the wings of aspect ratio 5.9 the wing tips were modified so that they remained parallel to the root chord and so that the taper ratio of the basic wing was retained. The wings of lower aspect ratio (3 and 2) were obtained by cutting off the wing in the plane parallel to the root chord at the required span. This decrease in aspect ratio resulted in an increase in taper ratio for the wings of aspect ratio 2 and 3. (See fig. 1.) The airfoil section used was a Rhode St. Genese 33 section perpendicular to the 0.50-chord line. This section

was used in accordance with free-flight-tunnel practice of using airfoil sections that obtain maximum lift coefficients in the low-scale tests approximately equal to the maximum lift coefficient of a full-scale wing having a conventional airfoil section.

The damping-in-roll and tuft tests were made in the Langley 15-foot free-spinning tunnel (reference 3) on a special stand which could be free in roll about the wind axis for damping tests or could be locked in roll for tuft tests. Figure 2 is a photograph of the stand as set up for rotation tests and figure 3 is a detailed sketch of the stand setup. The damping-in-roll and tuft tests were made at a dynamic pressure of 2.8 pounds per square foot, which corresponded to test Reynolds numbers of 209,000 and 243,000 based on mean aerodynamic chords of 0.68 feet and 0.79 feet for the wings of aspect ratios 5.9 and 2, respectively.

Force tests to determine the static aerodynamic characteristics of the wings were made on the Langley free-flight-tunnel six-component balance (reference 4), which rotates in yaw with the model so that all forces and moments are measured with respect to the stability axes. (See fig. 4.) These tests were made over the lift-coefficient range for angles of yaw of 0° and $\pm 5^\circ$ at a dynamic pressure of 3.0 pounds per square foot, which corresponds to test Reynolds numbers of 219,000 and 253,000 for the wings having aspect ratios of 5.9 and 2, respectively. The lateral stability characteristics were obtained from the runs at angles of yaw of $\pm 5^\circ$.

Values of the damping-in-roll parameter C_{l_p} and tuft-test studies were obtained for each wing through an angle-of-attack range which covered a lift-coefficient range from small positive lift coefficients through maximum lift coefficient.

The method of reference 1 was used to determine the damping in roll of the wings. This method consisted of steady-rotation tests on the roll stand (see figs. 2 and 3) and static rolling-moment tests. The stand and wing rotation was obtained by deflecting the vane ((1) shown in fig. 3). In steady rotation, the forcing moment was assumed to be equal to the damping moment and of opposite sign. The damping in roll of the stand and wing combination and of the stand alone were determined by recording the rate of rotation for several vane settings, both positive and negative. In order to determine the damping of the wing alone, the damping of the stand was subtracted from the damping of the stand and wing combination for any given rate of rotation.

RESULTS AND DISCUSSION

Force Tests

Figures 5 and 6 present the results of the force tests made to determine the lift, drag, and pitching-moment characteristics of the wings. The data of figure 5 indicate that reducing the aspect ratio of the swept-forward or swept-back wings resulted in a reduction in lift-curve slope in the range from low lift coefficients to moderate lift coefficients as is the case for unswept wings. These data also indicate that the swept-back wings reached greater maximum lifts than the swept-forward wings.

The pitching-moment data of figure 5 indicate that the swept-back and swept-forward wings having an aspect ratio of 5.9 are unstable at the stall. The large unstable pitching moments of these wings are caused by the loss in lift at the wing tips and root sections of the swept-back and swept-forward wings, respectively. These data also indicate that reducing the aspect ratio of either the swept-forward or swept-back wings tends toward stability at the stall. This trend is in agreement with the results presented in reference 5.

The lateral stability characteristics are presented in figure 6 in the form of plots of the lateral-force parameter C_{Y_β}, the effective-dihedral parameter C_{l_β}, and the directional-stability parameter C_{n_β} against angle of attack and lift coefficient. The following discussion of these data is concerned with the linear part of the lift curves unless otherwise noted. The data of figure 6 indicate that the transition from 42° sweepback to 38° sweepforward had a marked effect on C_{l_β} and C_{n_β} but little effect on C_{Y_β}. Over the linear range of the lift curve the swept-forward wings had zero directional stability ($C_{n_\beta} = 0$), whereas the swept-back wings had a definite increase in directional stability with lift coefficient above a lift coefficient of 0.3.

The data of figure 6 show that the swept-forward wings have negative effective dihedral (positive C_{l_β}), which becomes slightly more negative with increasing lift coefficient, and the swept-back wings have positive effective dihedral (negative C_{l_β}), which increases with lift coefficient. These data also indicate that sweepforward gives smaller negative values of effective dihedral at any

lift coefficient and smaller negative peak values than the positive values of effective dihedral obtained with sweepback. The maximum value of C_{l_β} for the swept-forward wings is approximately one-half of the maximum value of C_{l_β} for the swept-back wings. Over the greater part of the lift curve reducing the aspect ratio results in a more negative value of $-C_{l_\beta}$ for the swept-back wings and a smaller value of C_{l_β} for the swept-forward wings at any lift coefficient. The difference in the magnitude of the effective dihedral with sweepback and sweepforward and the effects of aspect ratio on the magnitude of the effective dihedral are explained in part in reference 6. Data from reference 6 show that reducing the aspect ratio of an unswept wing having an aspect ratio of 6 increases the effective dihedral in a positive direction. When the data of reference 6 are used with the data for swept wings to obtain incremental values of C_{l_β}, the change in C_{l_β} per degree of sweep appears to be approximately the same for sweepback and sweepforward.

Damping-in-Roll Tests

The results of the damping-in-roll tests are presented in figure 7. These data show that the damping-in-roll parameter C_{l_p} decreases at an increasing rate with lift coefficient for the swept-back wings and increases at an increasing rate with lift coefficient for the swept-forward wings up to a lift coefficient of 0.9. These data also show that up to a lift coefficient of 0.9, a reduction in aspect ratio results in a reduction in C_{l_p}. Over the linear range of each lift curve the magnitude of the change in C_{l_p} is approximately proportional to the change in lift-curve slope. (Reference 1 shows that C_{l_p} is a direct function of lift-curve slope and spanwise center of pressure). The slight variation in C_{l_p} over the linear range of the lift curve is probably the result of small spanwise shifts in center of pressure.

Autorotation at the stall was obtained only with the swept-back wing having an aspect ratio of 2. The trend toward instability in roll (autorotation) of the swept-back wings with a reduction in aspect ratio is attributed to the more abrupt stall as the aspect ratio is reduced. (See fig. 5.)

Because of the higher damping in roll of swept-forward wings, the present tests indicate that at moderate and high lift coefficients more effective ailerons would be required on swept-forward wings than would be required on swept-back wings to produce a given helix angle $\frac{pb}{2V}$. This problem may not be serious because it is expected that the flow changes that make the damping in roll greater will also increase the aileron effectiveness.

Tuft Tests

The results of tuft tests on the swept-back wings are presented in figure 8. These data indicate that reducing the aspect ratio of the swept-back wing from 5.9 to 3 and 2 did not alter the general flow pattern through the lift range below the stall. The reduction in aspect ratio resulted, however, in a more abrupt stall and in flow separation at the leading edge of the outboard region of each panel at the stall. In general the data of figure 8 show that for the swept wings at the low lift coefficients (up to a value of C_L of 0.5) the air flow over the upper surface of the wings is in the direction of the wind stream as over a conventional straight wing. At moderate lift coefficients (0.5 to 0.8) the air flow shows the tendency to move toward the wing tips along the trailing edge of the wing. As the lift coefficient is increased further, this outflow becomes more pronounced and affects chordwise stations progressively farther ahead of the trailing edge. At maximum lift and somewhat beyond maximum lift, all the flow is outward except at the root section, and only slight flow separation is indicated along the wing-tip leading edge.

The data of figure 9 indicate that for the swept-forward wings reduction in aspect ratio has very little effect on the general flow pattern throughout the lift range. At low lift coefficients (up to $C_L = 0.6$) the air-flow pattern appears similar to the flow pattern over a conventional straight wing except that a slight tendency to flow in toward the root section is noted along the trailing edge. As the lift coefficient increases, the inflow along the trailing edge becomes more pronounced and affects chordwise stations farther ahead of the trailing edge of the wing. At the same time the root section shows signs of separation of the flow at the trailing edge, which separation spreads forward and outward with increasing lift coefficient up to the stall.

CONCLUSIONS

The results of tests conducted in the Langley free-flight tunnel and Langley 15-foot free-spinning tunnel to determine the low-speed stability, damping-in-roll, and stall characteristics of five highly swept wings can be summarized as follows:

1. The swept wings of relatively high aspect ratio (5.9) were longitudinally unstable at the stall (nose-up pitching moments). Reducing the aspect ratio of the swept-back or swept-forward wings tended to eliminate this instability.

2. Sweepforward produced a maximum value of negative effective dihedral approximately one-half of the maximum value of positive effective dihedral produced by sweepback. Over the linear range of the lift curve the swept-forward wings had zero directional stability, whereas the swept-back wings had a marked increase in directional stability with lift coefficient above a lift coefficient of 0.3.

3. The damping in roll was reduced with reduction in aspect ratio over the linear range of the lift curve. Above the linear range of the lift curve the damping in roll decreased with increasing lift coefficient for the swept-back wings and increased with increasing lift coefficient for the swept-forward wings. Autorotation at the stall was obtained only with the swept-back wing having an aspect ratio of 2.

Langley Memorial Aeronautical Laboratory
National Advisory Committee for Aeronautics
Langley Field, Va., November 13, 1946.

REFERENCES

1. Bennett, Charles V., and Johnson, Joseph L.: Experimental Determination of the Damping in Roll and Aileron Rolling Effectiveness of Three Wings Having 2°, 42°, and 62° Sweepback. NACA TN No. 1278, 1946.

2. Maggin, Bernard, and Bennett, Charles V.: Flight Tests of an Airplane Model with a 42° Swept-Back Wing in the Langley Free-Flight Tunnel. NACA TN No. 1287, 1946.

3. Zimmerman, C. H.: Preliminary Tests in the N.A.C.A. Free-Spinning Wind Tunnel. NACA Rep. No. 557, 1936.

4. Shortal, Joseph A., and Draper, John W.: Free-Flight-Tunnel Investigation of the Effect of the Fuselage Length and the Aspect Ratio and Size of the Vertical Tail on Lateral Stability and Control. NACA ARR No. 3D17, 1943.

5. Shortal, Joseph A., and Maggin, Bernard: Effect of Sweepback and Aspect Ratio on Longitudinal Stability Characteristics of Wings at Low Speeds. NACA TN No. 1093, 1946.

6. Zimmerman, C. H.: Characteristics of Clark Y Airfoils of Small Aspect Ratios. NACA Rep. No. 431, 1932.

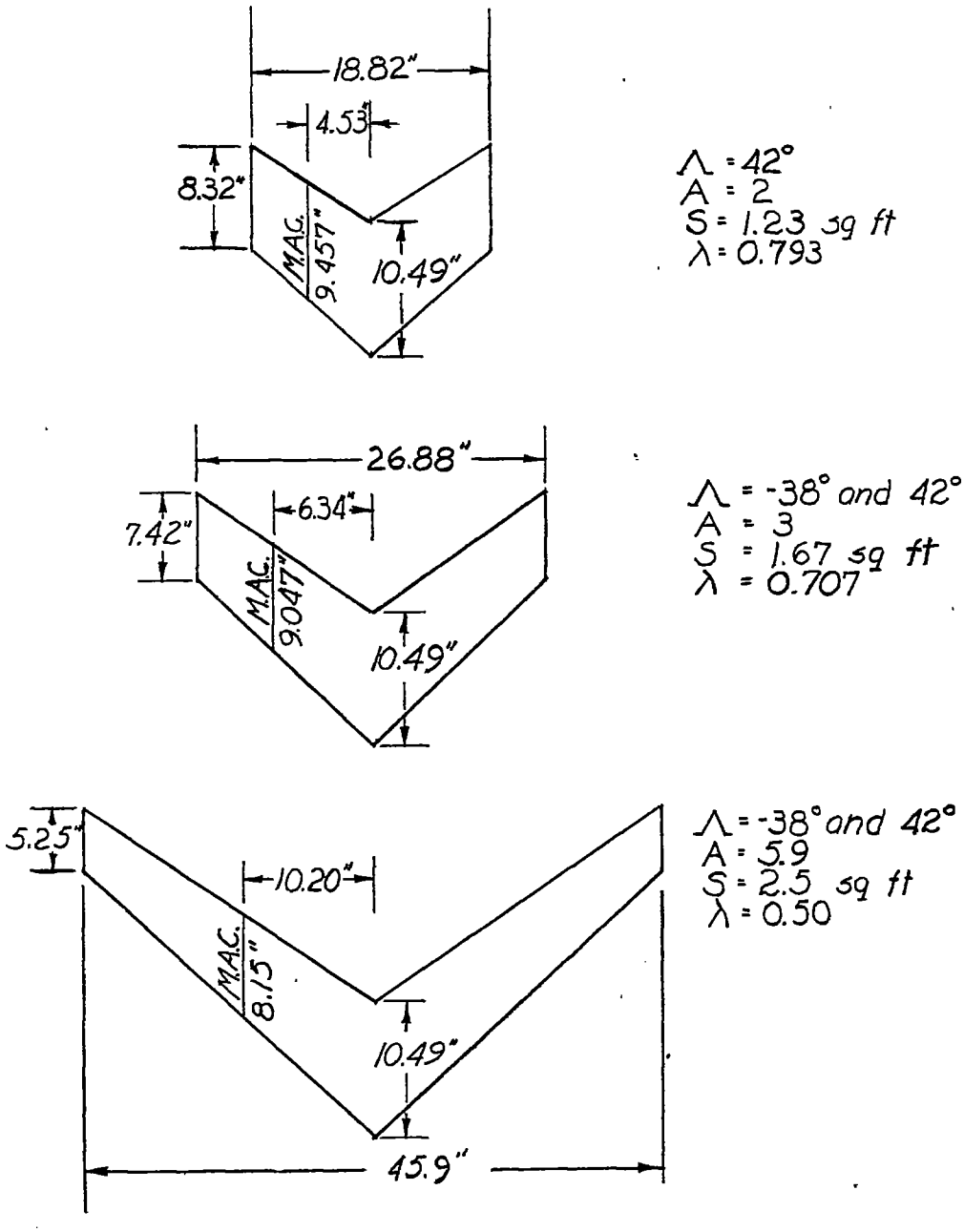

NATIONAL ADVISORY
COMMITTEE FOR AERONAUTICS.

Figure 1.- Sketch of wing planforms tested. All wings constructed with a Rhode St. Genese 33 airfoil section perpendicular to the 0.50-chord line.

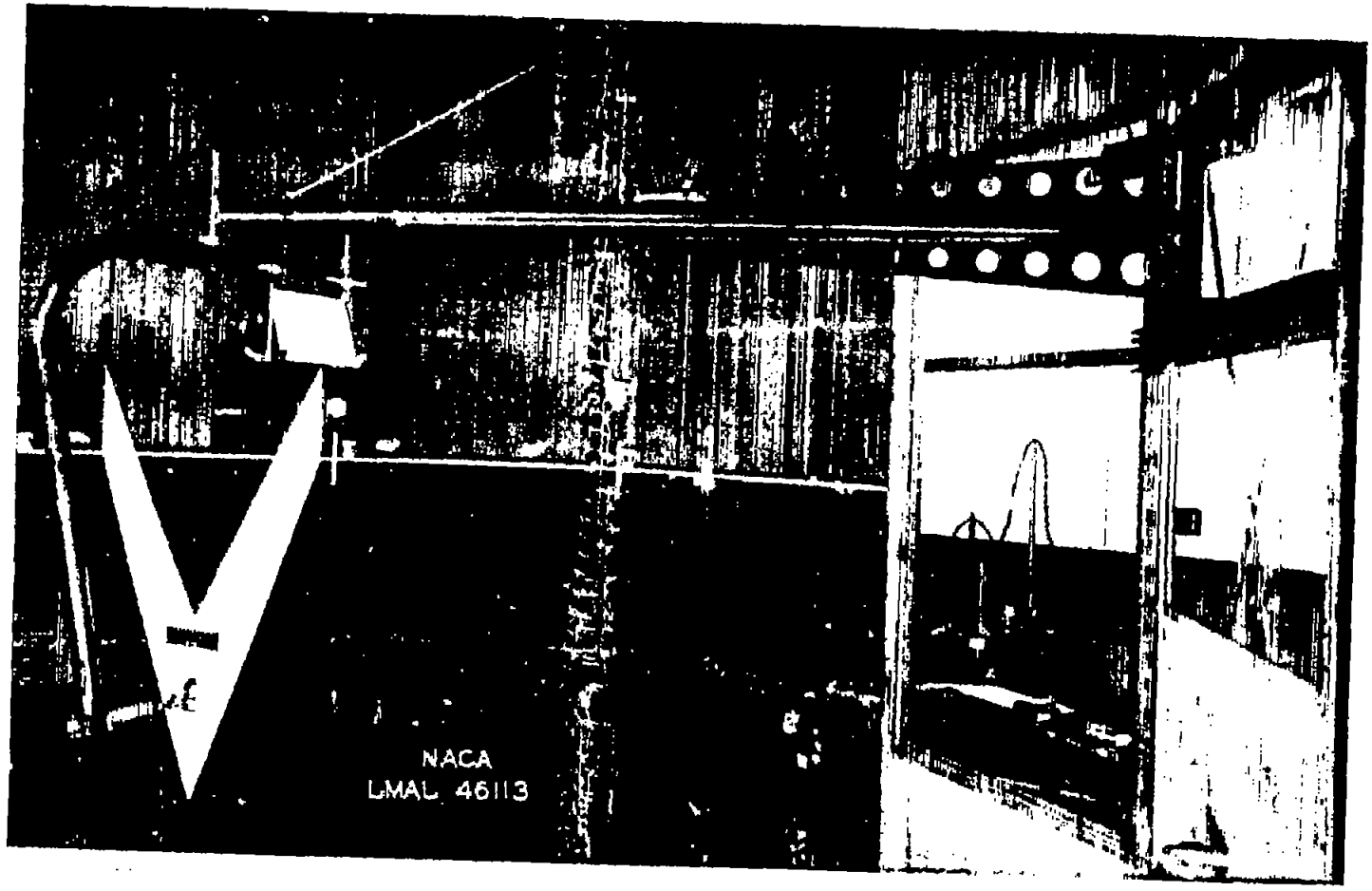

Figure 2.- Roll stand with model of swept-back wing attached, mounted in Langley 15-foot free-spinning tunnel.

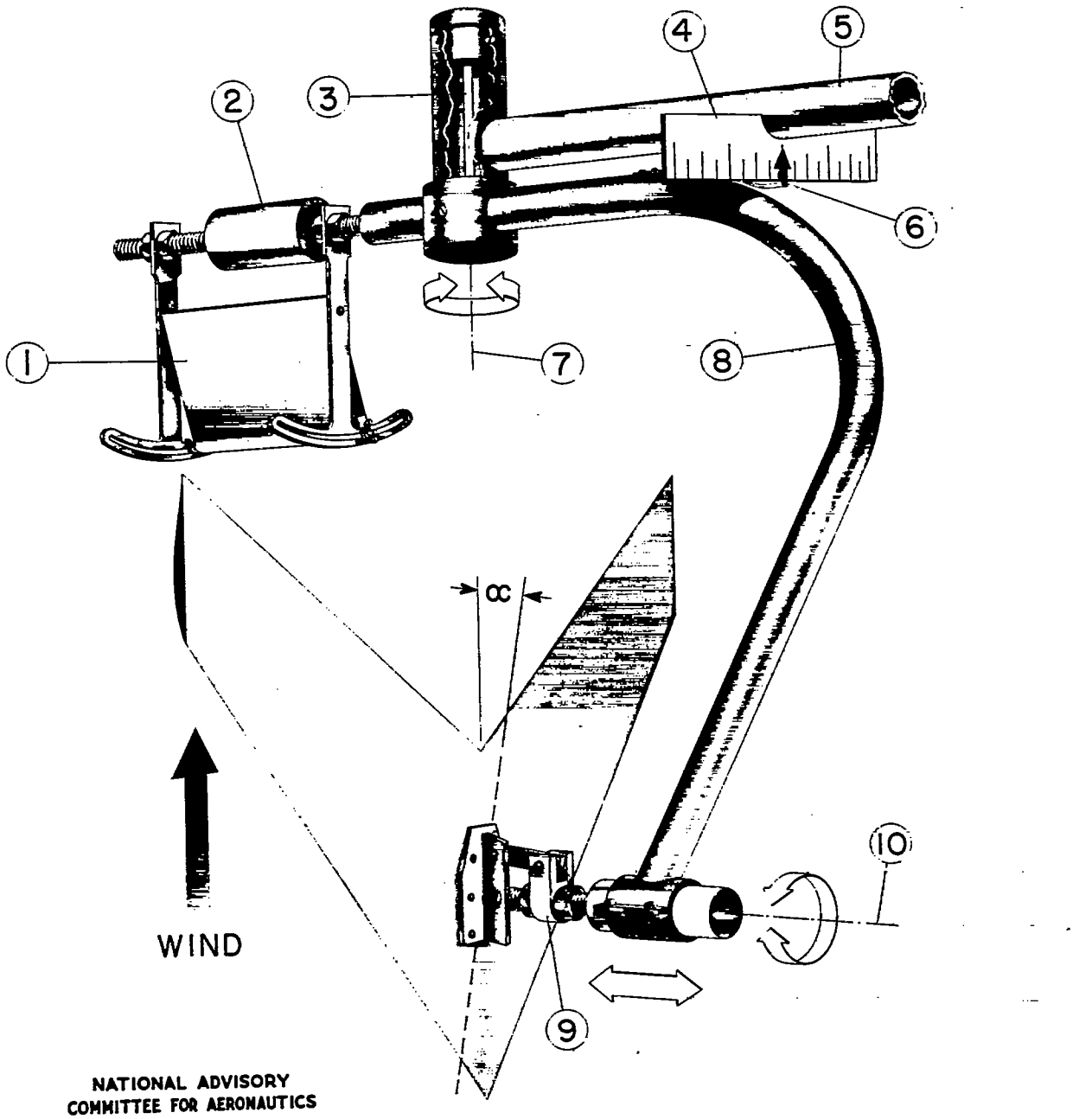

1 Vane (to produce rolling moment)
2 Counterweight
3 Torque rod (can be mounted in this head to measure rolling moment)
4 Scale (for reading torque-rod deflection in static tests)
5 Supporting arm (mounted to tunnel wall)
6 Pointer (to indicate torque-rod deflection in static tests)
7 Roll axis
8 Model support (can be free in roll or restrained by torque rod)
9 Mounting head (adjustable to desired angle of attack)
10 Yaw axis

Figure 3.- Roll bracket used to determine damping in roll.

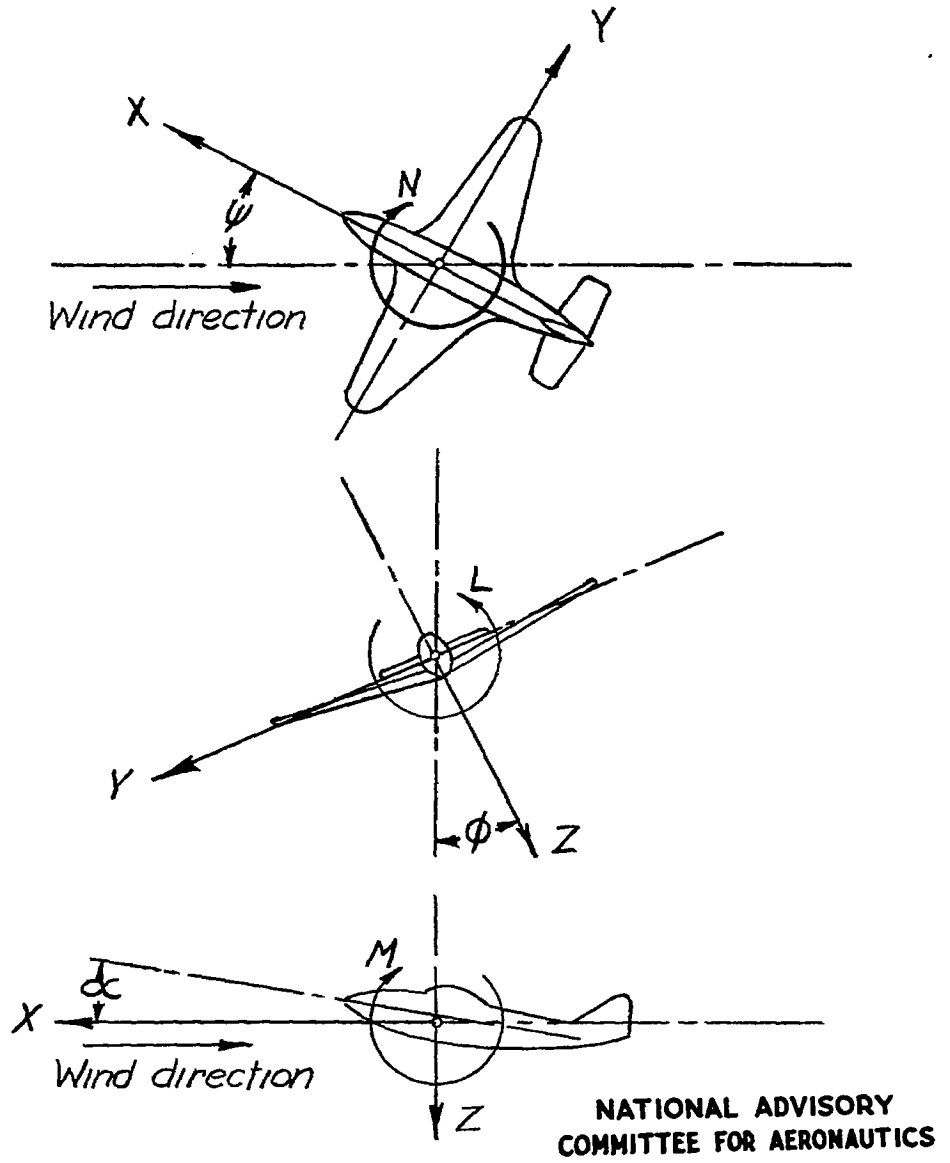

Figure 4.- The stability system of axes. Arrows indicate positive directions of moments and forces. This system of axes is defined as an orthogonal system having its origin at the center of gravity and in which the Z-axis is in the plane of symmetry and perpendicular to the relative wind, the X-axis is in the plane of symmetry and perpendicular to the Z-axis, and the Y-axis is perpendicular to the plane of symmetry.

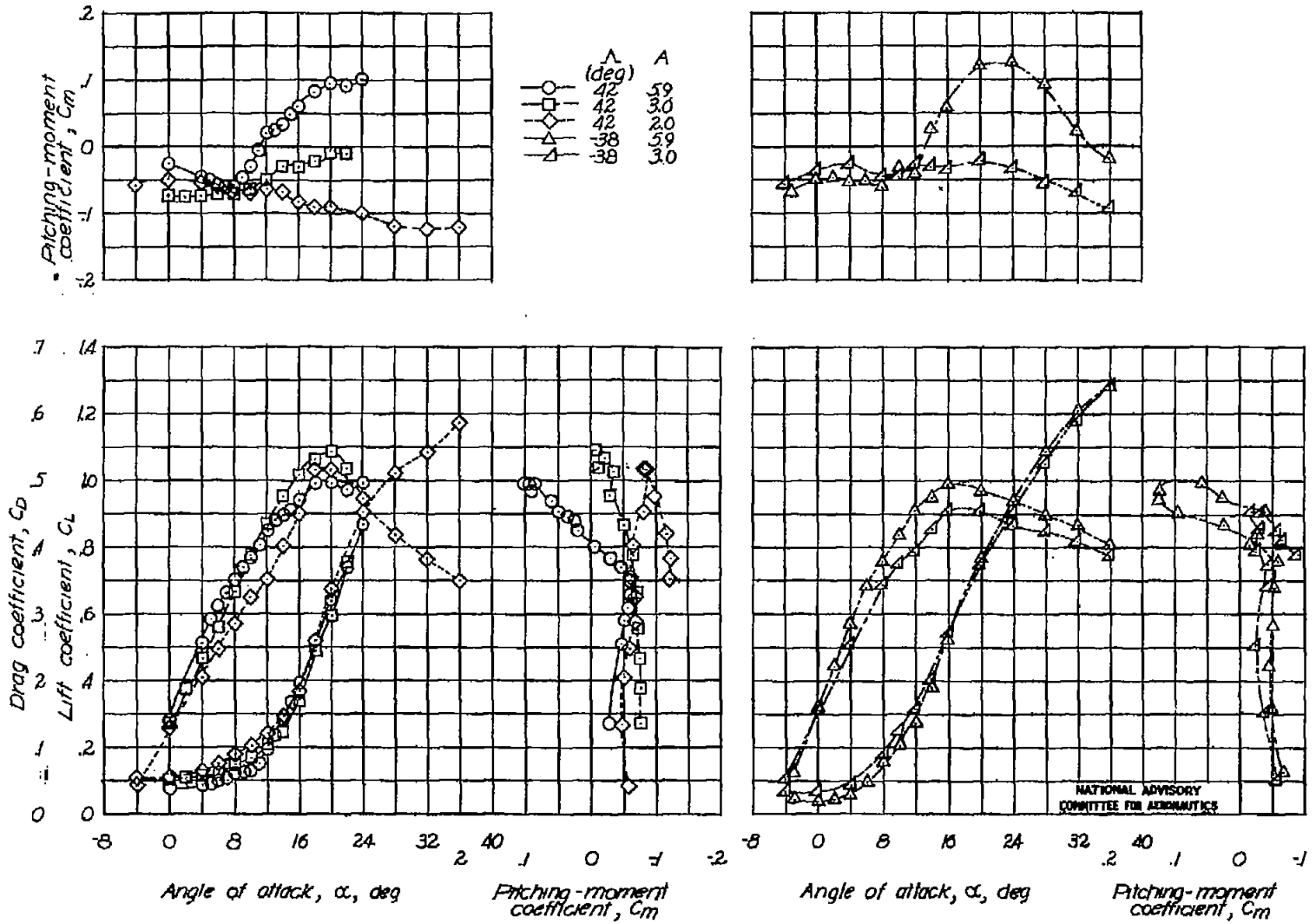

Figure 5.- Variation of the lift, drag, and pitching-moment characteristics with angle of attack for the wings tested. $q = 3.0$.

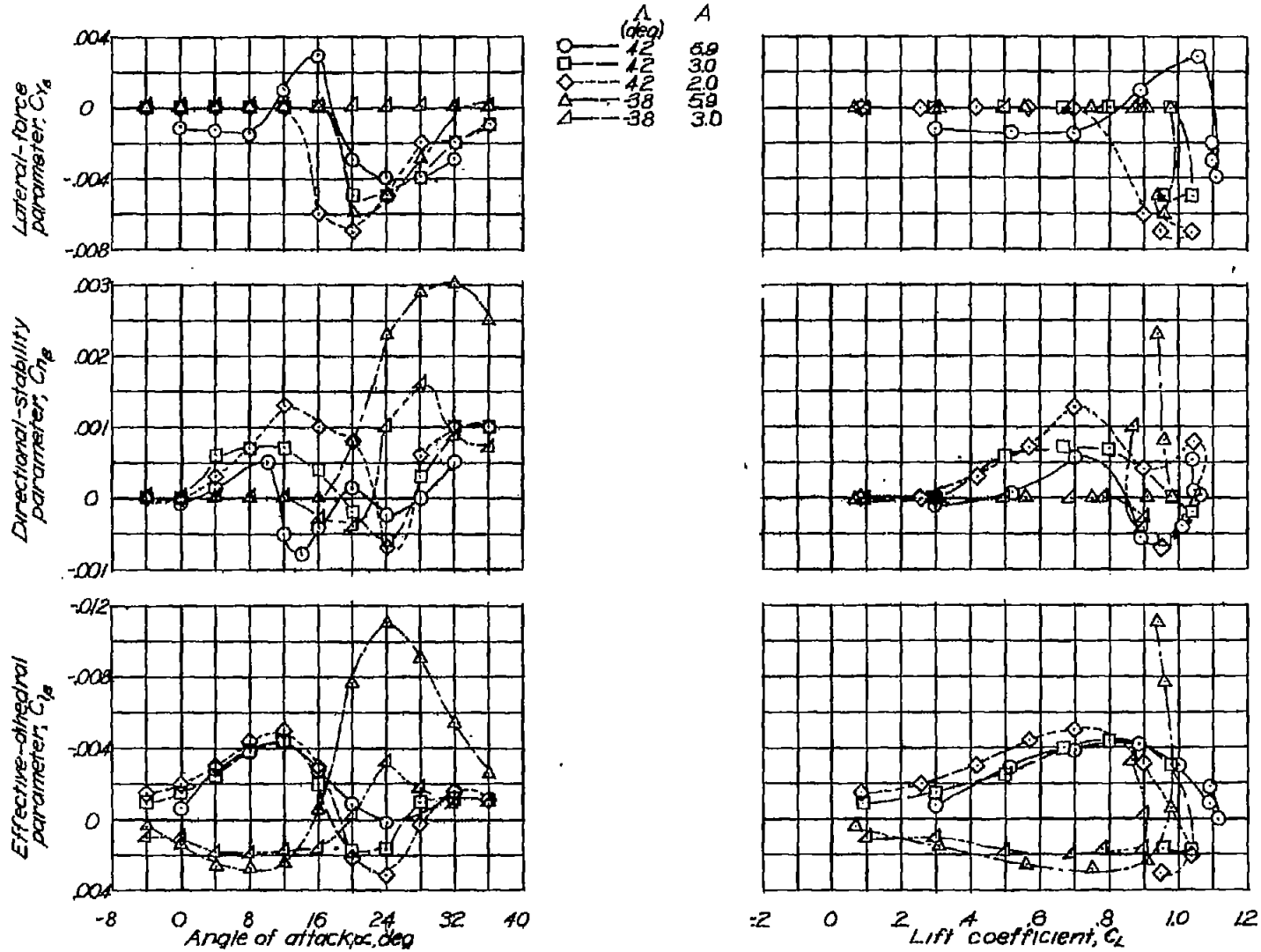

Figure 6. - Variation of the lateral-stability parameters C_{Y_β}, C_{n_β}, and C_{l_β} with angle of attack and lift coefficient for the wings tested.

NATIONAL ADVISORY COMMITTEE FOR AERONAUTICS

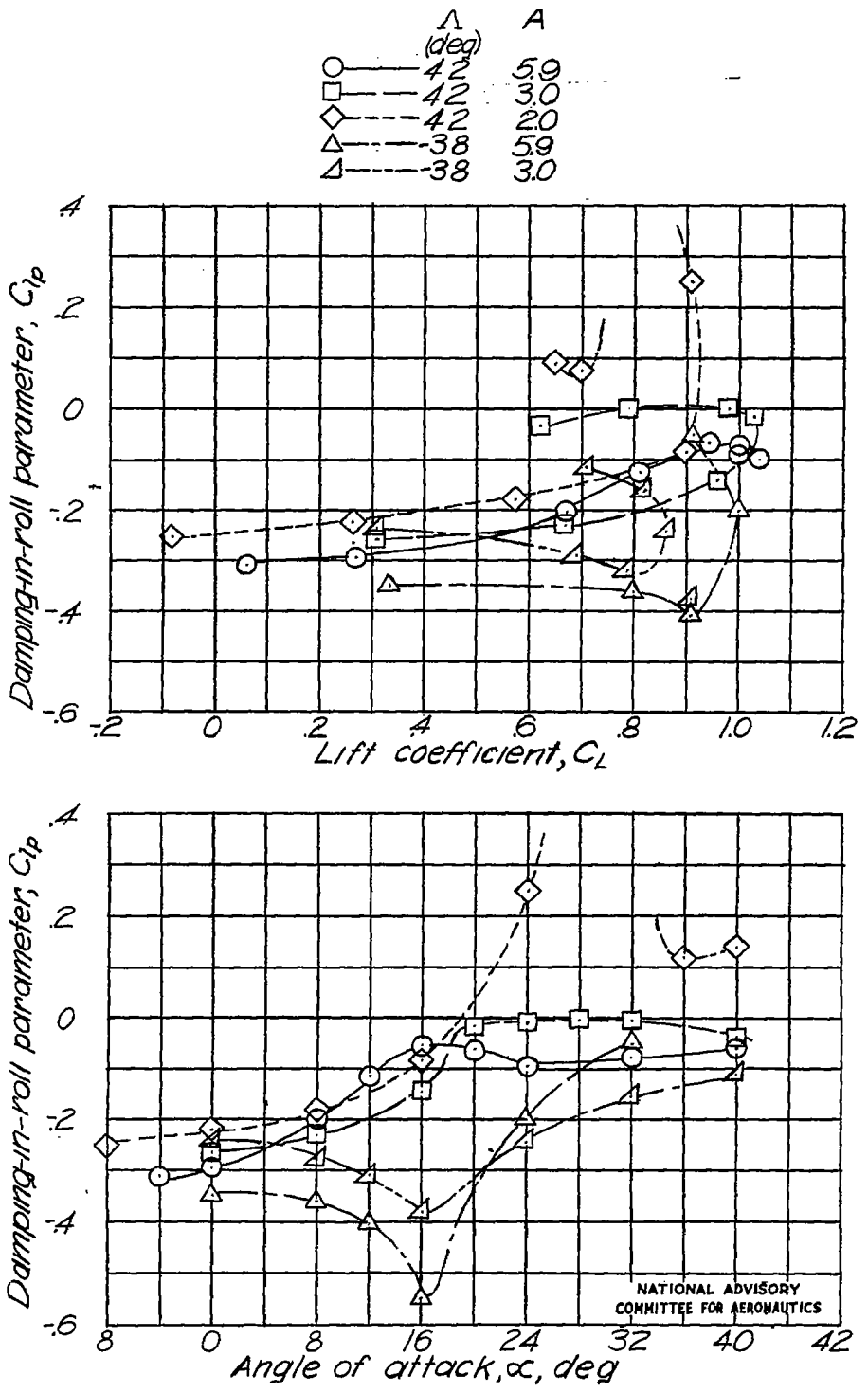

Figure 7.- Variation of the damping-in-roll parameter C_{l_p} with angle of attack and lift coefficient for the wings tested.

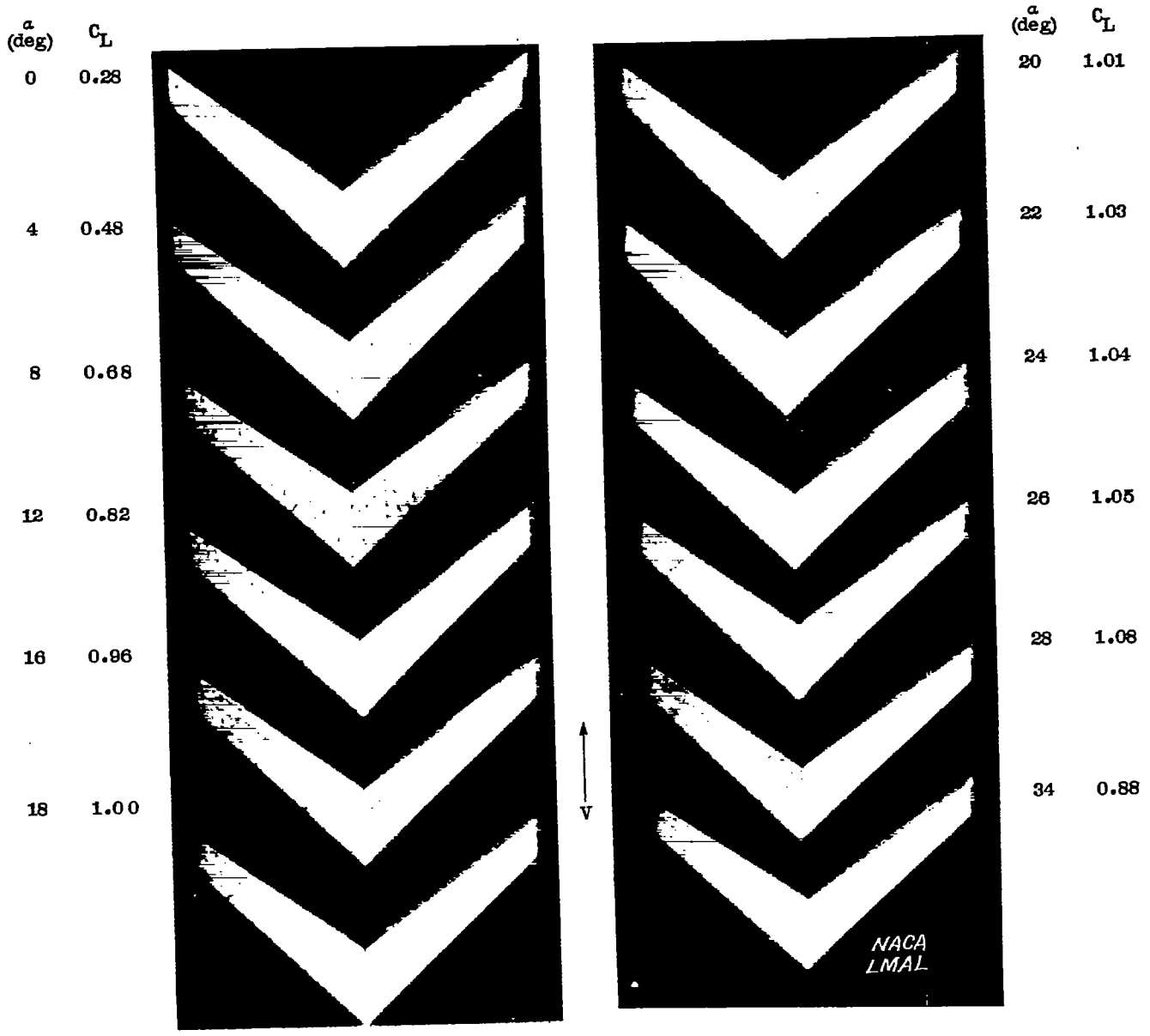

(a) A = 5.9; $\Lambda = 42^{\circ}$; $\lambda = 0.5$.

Figure 8.- Tuft studies of swept-back wings tested.

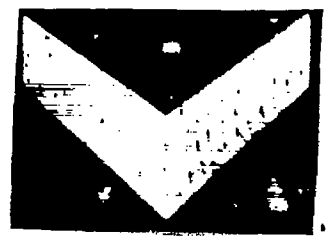

$\alpha = 0^{\circ}$, $C_L = 0.30$

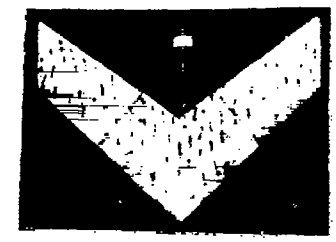

$\alpha = 10^{\circ}$, $C_L = 0.74$

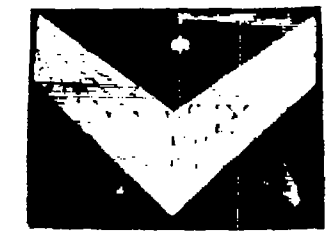

$\alpha = 18^{\circ}$, $C_L = 1.03$

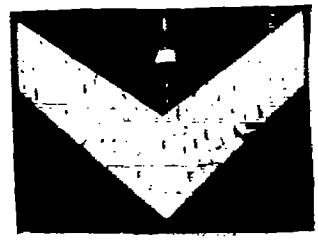

$\alpha = 4^{\circ}$, $C_L = 0.50$

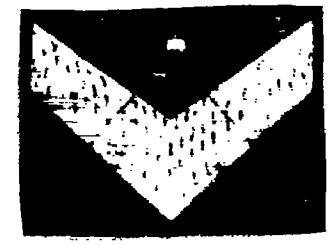

$\alpha = 12^{\circ}$, $C_L = 0.81$

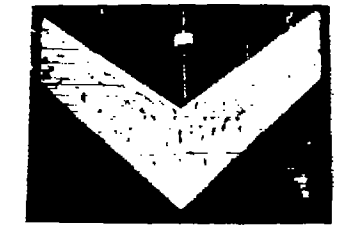

$\alpha = 20^{\circ}$, $C_L = 1.04$

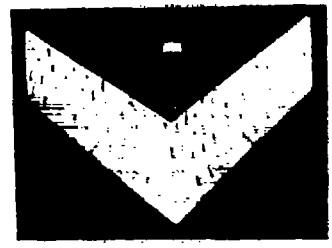

$\alpha = 6^{\circ}$, $C_L = 0.58$

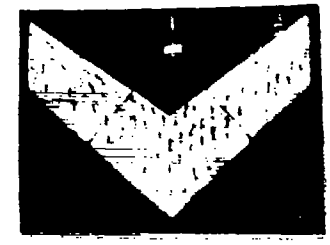

$\alpha = 14^{\circ}$, $C_L = 0.89$

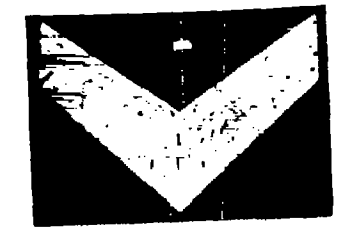

$\alpha = 22^{\circ}$, $C_L = 1.0$

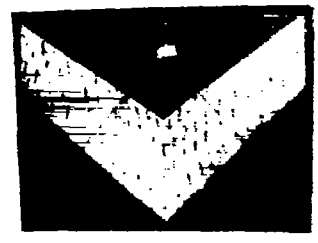

$\alpha = 8^{\circ}$, $C_L = 0.68$

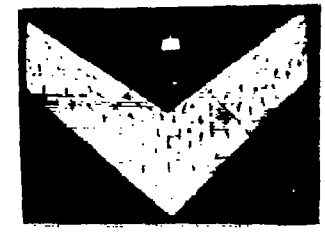

$\alpha = 16^{\circ}$, $C_L = 0.96$

$\alpha = 24^{\circ}$, $C_L = 0.96$

(b) $A = 3$; $\Lambda = 42^{\circ}$; $\lambda = 0.707$.

Figure 8.- Continued.

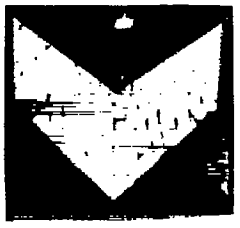

$\alpha = 0^{\circ}$, $C_L = 0.25$

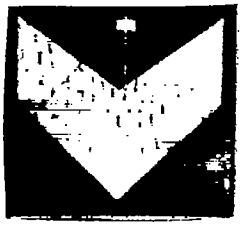

$\alpha = 10^{\circ}$, $C_L = 0.65$

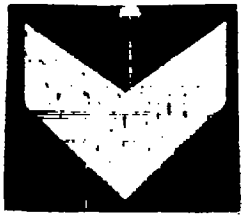

$\alpha = 18^{\circ}$, $C_L = 1.0$

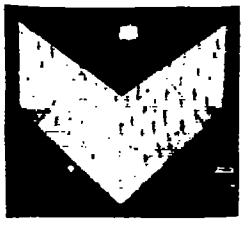

$\alpha = 4^{\circ}$, $C_L = 0.41$

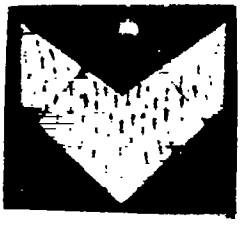

$\alpha = 12^{\circ}$, $C_L = 0.73$

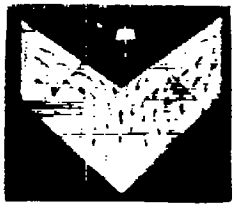

$\alpha = 20^{\circ}$, $C_L = 1.04$

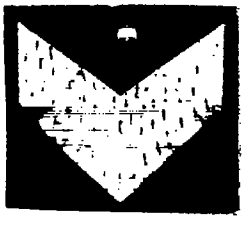

$\alpha = 6^{\circ}$, $C_L = 0.49$

$\alpha = 14^{\circ}$, $C_L = 0.80$

$\alpha = 22^{\circ}$, $C_L = 1.0$

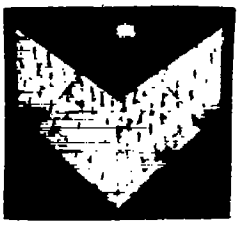

$\alpha = 8^{\circ}$, $C_L = 0.57$

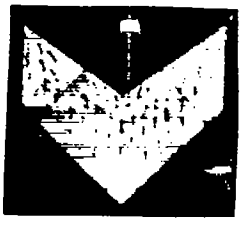

$\alpha = 16^{\circ}$, $C_L = 0.90$

$\alpha = 24^{\circ}$, $C_L = 0.96$

(c) $A = 2$; $\Lambda = 42^{\circ}$; $\lambda = 0.793$.

Figure 8.- Concluded.

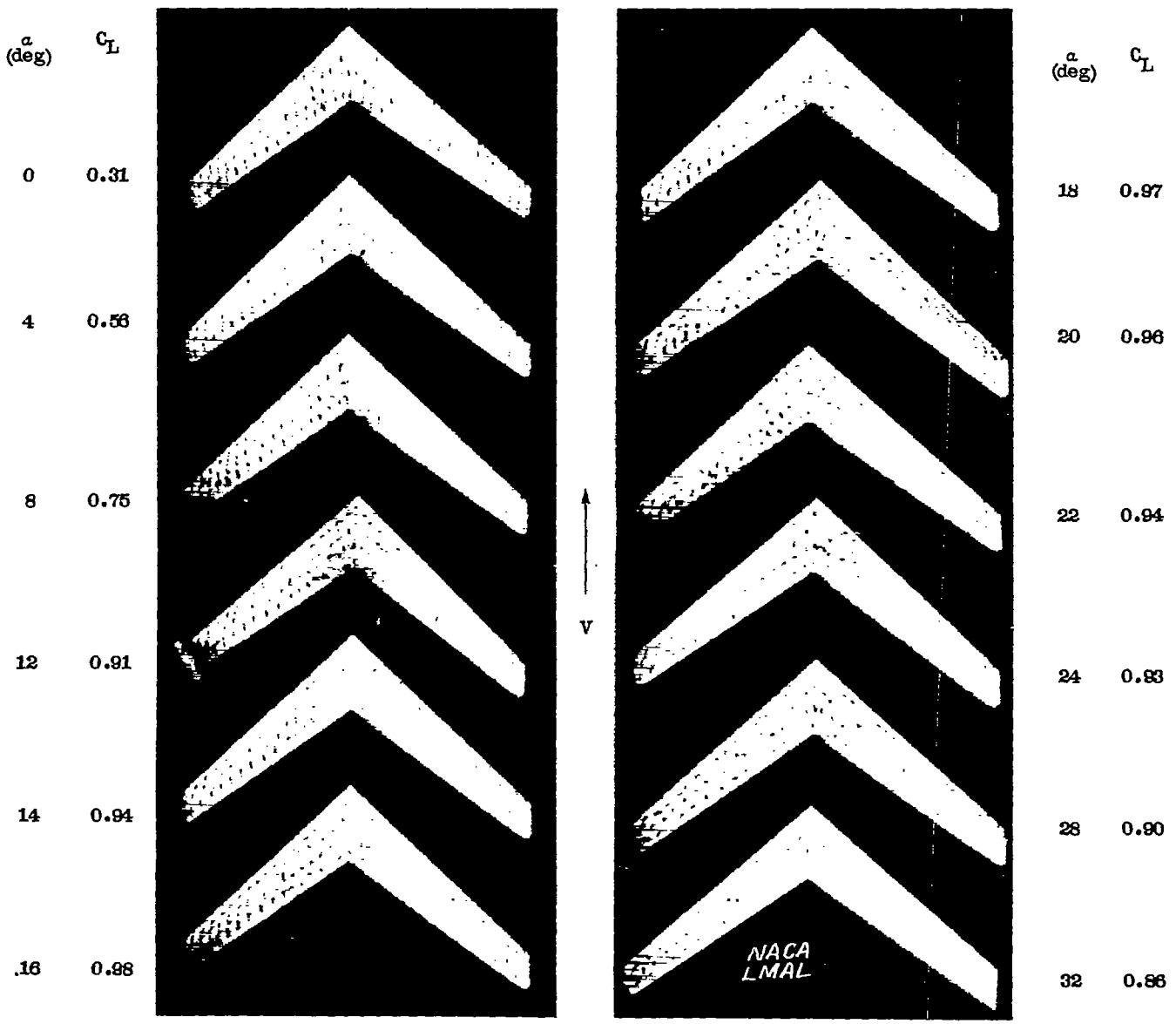

(a) A = 5.9; $\Lambda = -38^{\circ}$; $\lambda = 0.5$.

Figure 9.- Tuft studies of swept-forward wings tested.

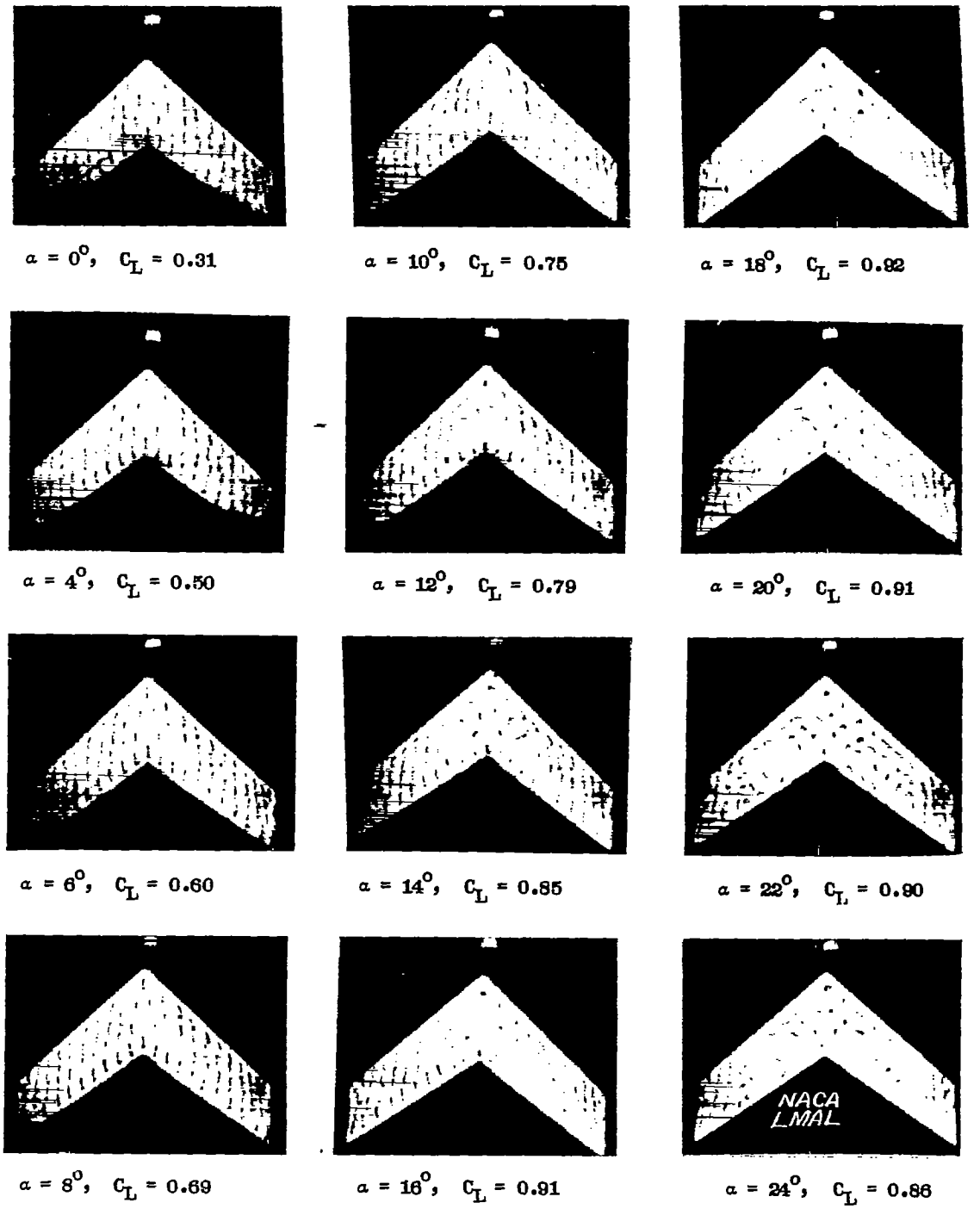

$\alpha = 0^{\circ}$, $C_L = 0.31$ $\alpha = 10^{\circ}$, $C_L = 0.75$ $\alpha = 18^{\circ}$, $C_L = 0.92$

$\alpha = 4^{\circ}$, $C_L = 0.50$ $\alpha = 12^{\circ}$, $C_L = 0.79$ $\alpha = 20^{\circ}$, $C_L = 0.91$

$\alpha = 6^{\circ}$, $C_L = 0.60$ $\alpha = 14^{\circ}$, $C_L = 0.85$ $\alpha = 22^{\circ}$, $C_L = 0.90$

$\alpha = 8^{\circ}$, $C_L = 0.69$ $\alpha = 16^{\circ}$, $C_L = 0.91$ $\alpha = 24^{\circ}$, $C_L = 0.86$

(b) $A = 3$; $\Lambda = -38^{\circ}$; $\lambda = 0.707$.

Figure 9.- Concluded.